

What is HDR? Perceptual Impact of Luminance and Contrast in Immersive Displays

Kenneth Chen
kennychen@nyu.edu
New York University, Meta
United States of America

Nathan Matsuda
nathan.matsuda@meta.com
Meta
United States of America

Jon McElvain
jmcelvain@meta.com
Meta
United States of America

Yang Zhao
yang.zhao@meta.com
Meta
United States of America

Thomas Wan
thomaswan@meta.com
Meta
United States of America

Qi Sun*
qisun@nyu.edu
New York University
United States of America

Alexandre Chapiro*
alex@chapiro.net
Meta
United States of America

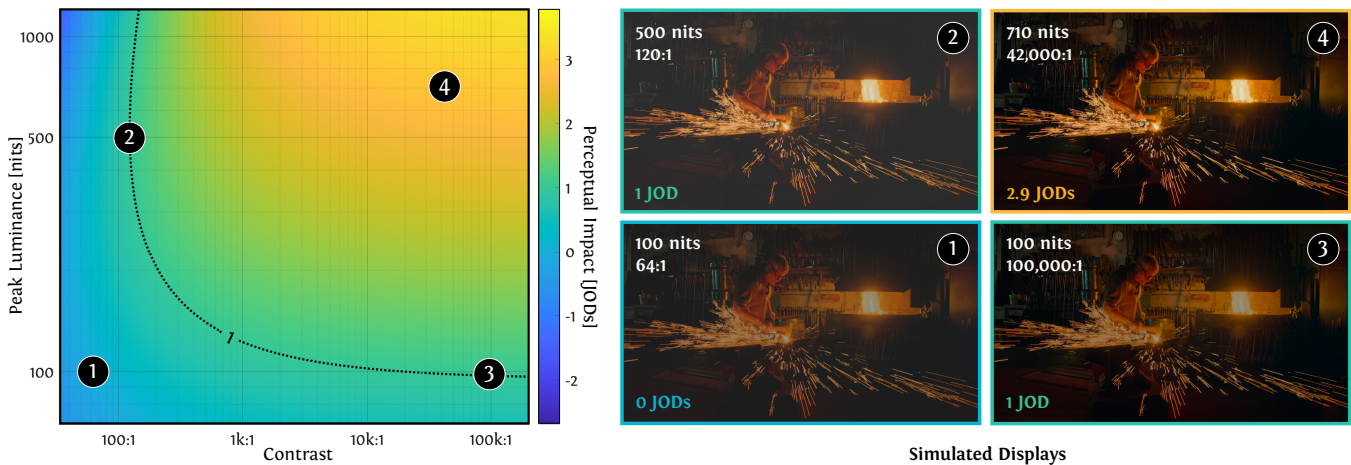


Figure 1: A model to predict perceptual impact (in Just-Objectionable-Differences, or JODs) is derived from HDR preference data for combinations of display contrast and peak luminance, with predictions visualized as a heatmap (left). In this plot, the baseline 0 JOD condition is set to values similar to commercially-available VR displays: 100 nits peak luminance and 64:1 contrast. In addition, we simulate three displays with different dynamic ranges. Our model allows us to examine the perceived improvement coming from increased peak luminance and contrast. For example, both display 2 and 3 provide a 1 JOD improvement over display 1. Note that HDR content cannot be displayed in a PDF format, so all images in this manuscript are tone-mapped for presentation. See supplementary webpage for representative content. Image credits HdM-Stuttgart.

Abstract

The contrast and luminance capabilities of a display are central to the quality of the image. High dynamic range (HDR) displays have high luminance and contrast, but it can be difficult to ascertain whether a given set of characteristics qualifies for this label. This is especially unclear for new display modes, such as virtual reality (VR). This paper studies the perceptual impact of peak luminance and contrast of a display, including characteristics and use cases representative of VR. To achieve this goal, we first developed a haploscope testbed prototype display capable of achieving a

nits peak luminance and 1,000,000:1 contrast with high precision. We then collected a novel HDR video dataset targeting VR-relevant content types. We also implemented custom tone mapping operators to map between display parameter sets. Finally, we collected subjective preference data spanning 3 orders of magnitude in each dimension. Our data was used to fit a model, which was validated using a subjective study on an HDR VR prototype head-mounted display (HMD). Our model helps provide guidance for future display design, and helps standardize the understanding of HDR¹.

CCS Concepts

- Computing methodologies → Virtual reality; Perception

Keywords

High Dynamic Range, Displays, Visual Perception, Virtual Reality

*corresponding authors.



This work is licensed under a Creative Commons Attribution 4.0 International License.
SIGGRAPH Conference Papers '25, Vancouver, BC, Canada
© 2025 Copyright held by the owner/author(s).
ACM ISBN 979-8-4007-1540-2/2025/08
<https://doi.org/10.1145/3721238.3730629>

¹Code, data, and supplementary content: kenchen10.github.io/projects/sig25/index.html

ACM Reference Format:

Kenneth Chen, Nathan Matsuda, Jon McElvain, Yang Zhao, Thomas Wan, Qi Sun, and Alexandre Chapiro. 2025. What is HDR? Perceptual Impact of Luminance and Contrast in Immersive Displays. In *Special Interest Group on Computer Graphics and Interactive Techniques Conference Conference Papers (SIGGRAPH Conference Papers '25), August 10–14, 2025, Vancouver, BC, Canada*. ACM, New York, NY, USA, 20 pages. <https://doi.org/10.1145/3721238.3730629>

1 Introduction

The dynamic range of a display is defined by the contrast between the brightest and darkest tones, from peak pixel activation to trough. High dynamic range (HDR) is a widely and commercially used term that describes displays supporting brighter whites and darker blacks. As such, HDR is commonly defined by contrast and peak luminance, although color gamut, bit depth, gamma, and other characteristics are also often discussed in this context.

Much of the work defining today's HDR standards was done with cinematic applications in mind. However, as display technologies grow more and more complex, the applicability of these results may be jeopardized. This is true for new display architectures, like zonal or pixel-level dimming, but even more critical for emerging display modes, such as VR. VR displays have limited dynamic ranges when compared to traditional displays: battery limitations and the presence of optical elements preclude them from producing high brightness and reduce contrast. Furthermore, content viewed on VR displays is often of a different type than what is shown in movies, and may benefit from peak luminance and contrast differently.

Existing definitions for HDR classification often rely on empirical industry standards. Previous research efforts have probed user preferences for HDR, but there is nevertheless little quantitative data to model perceived quality. In this work, we establish the first unified preference scale for dynamic range. In particular, we focus on the weighed tradeoffs between the two core factors determining HDR: peak luminance and contrast.

To this aim, we first developed a haploscopic testbed that allows for significantly more dynamic range than what would typically be possible in commercially available VR displays. Leveraging our testbed, we conducted a large-scale psychophysical study using HDR video stimuli representative of typical use cases in VR. Content was mapped between dynamic ranges using one of two tone mapping schemes. The study results are used to create a model that maps display contrast and peak luminance to user preference scores, scaled in Just-Objectionable-Difference (JOD) units. Finally, an evaluation study conducted on an HDR VR prototype shows our model's ability to generalize to a headmounted VR scenario. Our research sets the targets for future VR HDR display designs and applications, helping guide hardware and software for perceptually efficient HDR displays. In summary, our contributions are:

- a reliable experimental setup, including an HDR testbed and psychophysical processes required to obtain accurate measures of HDR preference;
- a dataset of HDR content encompassing VR use cases, spanning different peak luminance and contrast values via custom tone mapping operators, rated with user preference scores in absolute JOD units;

- a computational model fit to this data that predicts perceptual quality given the display's peak luminance and contrast;
- a series of practical applications such as optimizing HDR display design and power consumption.

2 Related Work

Industry standards define HDR (Section 2.1), but do not necessarily align with the human visual system's abilities (Section 2.2), or with subjective preferences in HDR (Section 2.3).

2.1 What is HDR, today?

HDR is a popular label for displays, including commercially available televisions, phones and monitors. Although many possible definitions for what makes a display HDR exist, such as the capacity to play content in HDR file formats, we are interested specifically in a display's ability to reproduce contrast and luminance.

Consumer-facing review websites sometimes provide uninformative product evaluations – for instance, RTINGS.com² defines the contrast of any OLED display as infinite³. The Video Electronics Standards Association's (VESA) DisplayHDR⁴ standard defines a tier list of parameters including peak luminance, black level, contrast, etc. required for certification by this group. However, no perceptual rationale for how tiers are set is given. Ward [2008] proposed that VESA's definition of dynamic range is insufficient, as it ignores factors like ambient light, quantization, etc., and criticized contrast ratio as a means to perceptually describe HDR.

This is further complicated when discussing new technologies for which no standards exist. An example are VR displays which contain optical elements that may introduce blur or reduce contrast [Mantiuk et al. 2024] in a content-dependent manner.

2.2 Luminance Perception

The human visual system (HVS) is able to distinguish light over 14 orders of magnitude [Ferwerda 2001; Spillmann and Werner 2012]. Several works studied threshold HVS responses to simple luminance and contrast stimuli. Kunkel and Reinhard [2010] studied the ratio between the brightest and darkest features detectable by the HVS in a given adaptative state, finding it to be at least 3.7 log nits. Radonjić et al. [2011] studied a mapping between luminance and lightness for checkerboard patterns under varying ambients, finding the HVS capable of scaling lightness over 3+ log units of luminance. Vangorp et al. [2015] conducted studies to model the effect of adaptative state on local luminance detection. Contrast constancy [Kulikowski 1976] and the Ferry-Porter law [Ferry 1892; Porter 1902] have been shown to break down across large luminance ranges [Ashraf et al. 2022; Chapiro et al. 2023]. Rather than focusing on the absolute limits of threshold vision, our paper focuses on preferences for HDR content depiction at practically relevant luminances and contrasts.

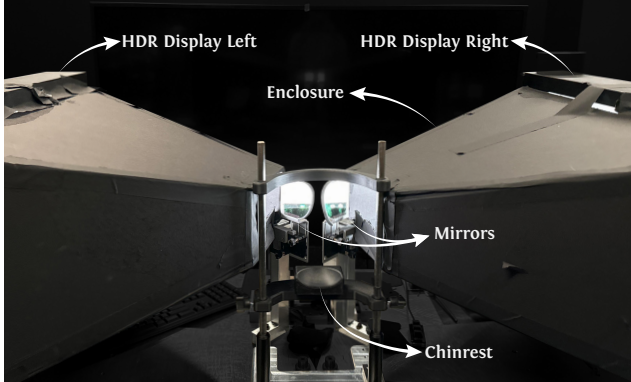
2.3 User Preference in HDR Displays

Several works studied dynamic range requirements of HDR displays in terms of user preference. Mantiuk et al. [2010] studied the black

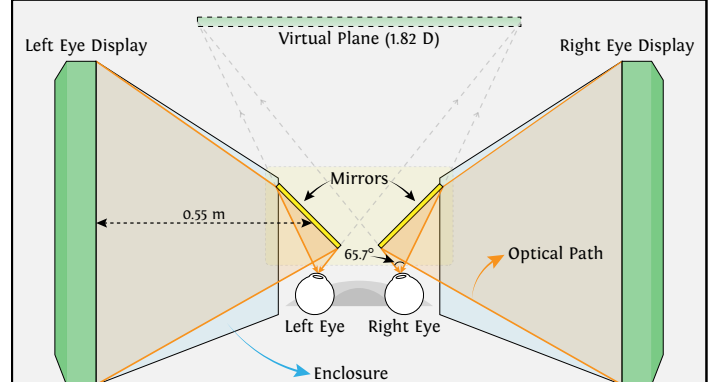
²RTINGS.com

³Sony A95L OLED TV Review

⁴displayhdr.org



(a) photograph of the haploscope testbed



(b) top-down schematic

Figure 2: Haploscope display system. To study varying contrast and peak luminance parameters, we need a display system that can reproduce a wide dynamic range. (a) We built a hardware testbed, which includes two HDR displays, one for each eye. Light from the displays reflects off of mirrors (>98% reflectance) toward the user, whose head is stabilized by a chinrest. (b) Top-down schematic showing the optical paths. The virtual image is presented at 1.82 diopters.

level required to match “absolute black”, finding 0.0044 nits sufficient for a dark surround and up to 1 nit for a very bright surround. Wanat et al. [2012] followed up, finding the highest perceivable contrast for their setup between 1,300:1 and 2,400:1.

Many studies focused on HDR for traditional displays. Akyüz et al. [2007] found HDR presentation superior to SDR, with brightness taking precedence over dynamic range. Using a prototype HDR display Seetzen et al. [2004, 2006] found higher peak luminances improve quality regardless of contrast, up to a point. Rempel et al. [2009] showed that under bright ambient light, users prefer higher peak luminances, but choose the lowest black level regardless of ambient. The Dolby study [Daly et al. 2013] had a heavy focus on cinema, going as far as simulating exit sign lighting in the study setting. The authors found that a black level of 0.1 nits and peak luminance of 650 nits satisfied the average user; a separate study on highlights required a peak luminance of up to 18,000 nits. Related variables, such as color gamut size [Park and Murdoch 2020] and display distance [Hammou et al. 2024] were also explored.

Viewing conditions in VR differ from traditional display, affecting user preferences. Depth judgements in stereo VR are modulated by contrast and luminance changes [Wolski et al. 2022], and display field of view has a significant effect on perceived brightness [Chapiro et al. 2018]. Matsuda et al. [2022a] demonstrated an HDR VR prototype capable of luminances over 20,000 nits. A subjective study was presented using scans of real-world environments, showing user luminance preferences exceed the capabilities of commercially available devices, particularly for outdoor scenes.

Despite these results, no unified perceptual scale defining preferences across peak luminance and contrast in HDR displays exists. We set out to build such a scale, shown in Figure 1 (left), by measuring subjective preference in VR using relevant content.

3 Experimental Methods

The goal of our study is to determine the perceptual impact of contrast and peak luminance in VR displays. Section 3.1 describes the experimental hardware, capable of reproducing a wide luminance and contrast range. Section 3.2 details how displays with a compressed dynamic range were simulated using tone mapping. Section 3.3 presents our experimental dataset of HDR videos. Finally, Section 3.4 describes the study itself.

3.1 Hardware Testbed

Contrast in modern VR headsets is limited due to the presence of optical components in the visual path. Notably, even custom HDR VR displays have simultaneous contrast lower than 100:1 [Matsuda et al. 2022b]. This differs from traditional displays, where a budget television may have contrast over 5000:1, while high-end models often go over 380,000:1 (see Supplement I for examples).

To overcome this challenge, we built a custom stereoscopic haploscope testbed (see Fig. 2a) using two 4K resolution, 60 Hz frame rate, 10 bit, 31.1" EIZO ColorEdge PROMINENCE CG3146⁵ professional HDR reference monitors, with a contrast ratio of 1,000,000:1 and peak luminance of 1,000 nits. Light from each display is reflected by a mirror (Edmund Optics protected silver) with reflectance greater than 98%, enabling peak luminance of 980 nits. The system’s field of view is 65.7°, in line with VR prototypes [Matsuda et al. 2022b]. A schematic is shown in Figure 2b, and details related to calibration, optical arrangement, and more can be found in Supplement D.

3.2 Display Simulation

To study different display dynamic ranges, we must be able to present content as it would be seen on a display with target reduced contrast and peak luminance. This is accomplished via tone

⁵EIZO CG3146 specifications: eizo.com/products/coloredge/cg3146

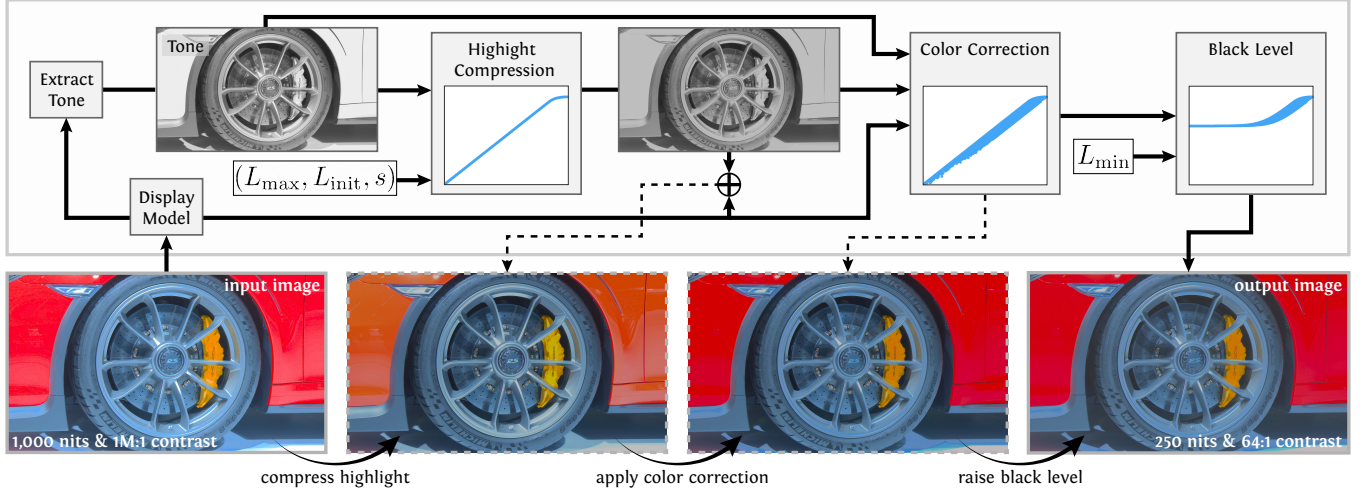


Figure 3: Steps of our display simulation algorithm. A frame is fed to a display model, which outputs the luminance values emitted by the display device. The tone of the output linear image is extracted, and its highlight is compressed via Chen et al. [2023]. To maintain color ratios, Schlick [1995] color correction is applied. Finally, the black level of the display is raised to produce the output frame. Here, the target display has peak luminance 250 nits & 64:1 contrast. Image credits SJTU.

mapping operators (TMOs) - algorithms that serve to convert content to a different (typically smaller) dynamic range, while aiming to preserve the original scene's look [Tumblin and Rushmeier 1993]. Because this is a compression operation, the result is typically lossy in terms of visible quality. Many TMOs have been proposed in the literature [Eilertsen et al. 2017], and evaluating their merits is outside the scope of this work.

While TMO choice will have an effect on preference for display characteristics, our goal is not to determine an optimal tone mapping scheme. We selected a curve formulation given by Chen et al. [2023], which is similar to the International Telecommunication Union (ITU) standard recommendation for HDR TV [Series 2019]. The shape of the curve is illustrated in Figure 3 (*Highlight Compression*), and reduces the contrast of highlights via a smooth rolloff spline, which begins at a luminance L_{init} , with smoothness s .

To demonstrate that tone mapping algorithm implementation may have a non-trivial impact on visual quality we employed two implementations using a modified version of this curve. The first employs a simple content-independent instance. Throughout this paper, we refer to this TMO as **FIXED TMO**. Secondly, we make this TMO content-adaptive (**CONTENT-AWARE TMO**) by using the VR TMO optimization framework of Tariq et al. [2023].

3.2.1 FIXED TMO. Our process of implementing the tone mapper consisted of these steps in order of application (shown in Figure 3):

1. **A display model** converts a display-encoded frame \mathcal{F} to linear values, $\mathcal{I} = \mathcal{E}(\mathcal{F})$, where $\mathcal{E}(\cdot)$ is the perceptual quantizer (PQ) electro-optical transfer function (EOTF) [Miller et al. 2013]. Similar to SDR gamma (e.g. sRGB), PQ is a transfer function for HDR content that maps luminance up to 10k nits.
2. **Tone extraction** by computing per-channel maximum of the linear RGB image \mathcal{I} ,

$$\mathcal{T} = \max (\mathcal{I}_r, \max (\mathcal{I}_g, \mathcal{I}_b)), \quad (1)$$

where $\mathcal{I}_r, \mathcal{I}_g, \mathcal{I}_b$ are the red, green, and blue channels of the input image, respectively. An image's *tone* \mathcal{T} is a proxy for relative luminance, which is commonly the component used in tone mapping [Reinhard et al. 2002]. Operating on tone rather than luminance avoids out-of-gamut colors after color correction (see Supplement Section A.1).

3. **Highlight compression** applying the tone curve [Chen et al. 2023] on \mathcal{T} . Two constants, a starting luminance L_{init} and a smoothness parameter s , define the shape of the curve. Tone values less than L_{init} are unmodified. High values of s are closer to a log-linear curve, and low values nearer to clipping.

4. **Color correction** using the Schlick [1995] formula,

$$\mathcal{I}' = \frac{\mathcal{T}'}{\mathcal{T}} \mathcal{I}. \quad (2)$$

Tone mapping can alter color appearance, and we apply this correction to preserve color ratios. Figure 3 (bottom, 2nd image) shows the result without this correction, where the color of the scene differs significantly from the input.

5. **Black level addition**, simulating low contrast displays as described by Mantiuk et al. [2024] and Chapiro et al. [2024], is done by raising the minimum luminance L_{min} , of the hypothetical display through an ambient term:

$$\mathcal{I}_{\text{mapped}} = \left(\frac{L_{\text{max}} - L_{\text{min}}}{L_{\text{max}}} \right) \mathcal{I}' + L_{\text{min}}. \quad (3)$$

We implemented this TMO with structure similar to Algorithm 1. In Section 5.1, we demonstrate a real-time shader implementation.

- 3.2.2 CONTENT-AWARE TMO.** Tariq et al. [2023] built an optimization framework targeted for HDR VR, which aims to compute the TMO parameters that minimize contrast distortion. We employed this framework, modifying Step 3 of the **FIXED TMO**, to optimize the curve's starting luminance L_{init} . A heuristic computation was used for the smoothness parameter s (see Supplement Section A.2).

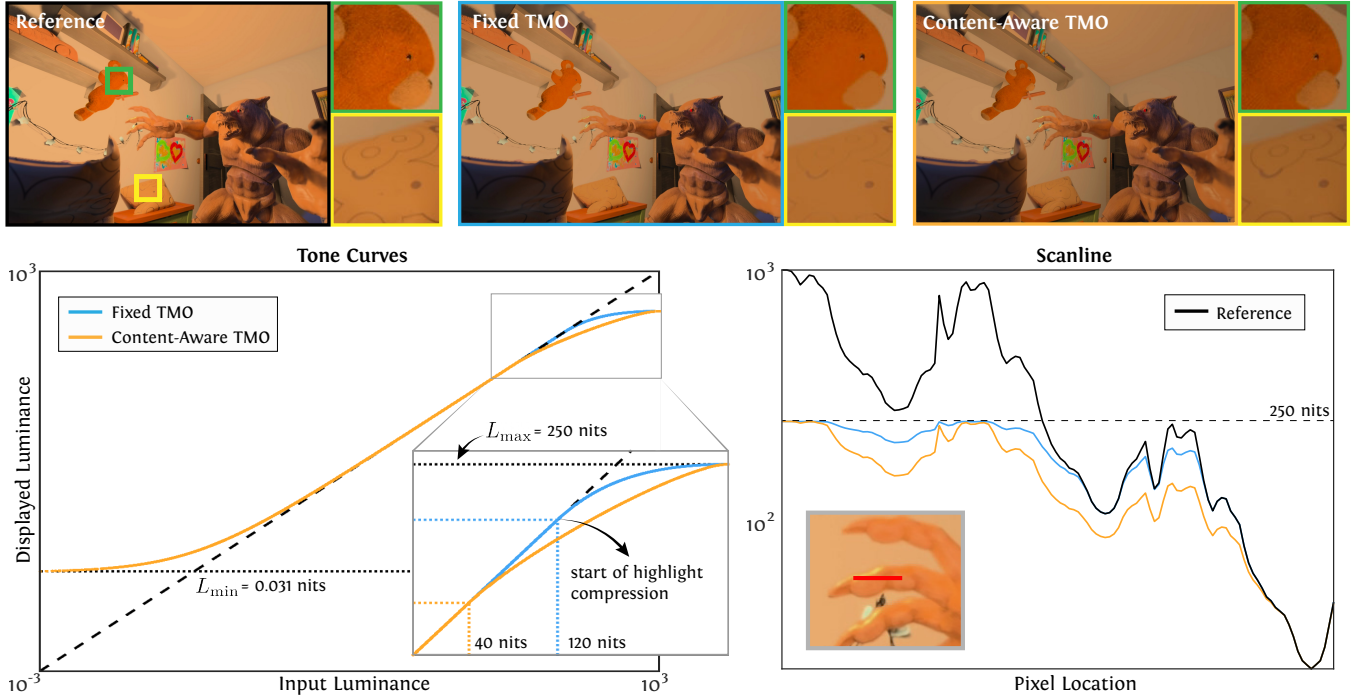


Figure 4: A comparison of tone curves. We compare the two tone curves used in our perceptual study, the **FIXED TMO** and the **CONTENT-AWARE TMO**, through visual example (top). Zoomed insets are displayed to the right of each image. Here, content is mapped to 250 nits peak luminance and 8,000:1 contrast (0.031 nit black level). The shape of each tone curve is visualized in the plot at bottom left, where the x -axis presents the luminance of the source frame and the y -axis shows the luminance of the mapped result. See the zoomed inset; the starting luminance of highlight compression is optimized in the **CONTENT-AWARE TMO**. A luminance scanline (measured at the red line on a zoom-in of the werewolf’s hand) is shown on the bottom right.

Following Tariq et al. [2023], we apply a leaky integrator to the optimized key value to improve temporal stability.

A comparison of the two TMOs is shown in Figure 4. In the qualitative example, the insets show a case in which the heuristic starting value selected for the **FIXED TMO** clips details which are visible in the **CONTENT-AWARE TMO**. The **CONTENT-AWARE TMO** starts highlight compression at a lower luminance than the **FIXED TMO** (Figure 4, bottom left), but contrasts are preserved as shown in the scanline plot. For pseudocode, see Supplement Section A.4.

3.3 Constructing an HDR-VR Video Dataset

Most prior preference studies in HDR (Sec. 2.3) focused largely on cinema and home theater applications – targeting “cinematic” content, or used HDRI probes captured in real-world environments for VR [Matsuda et al. 2022a]. Our work focuses on VR HDR, and as such we aim to use content that is representative of typical VR use cases. Our stimuli focus on four categories spanning major VR use cases. Namely, this includes productivity (scrolling the web, messaging), faces (augmented calling), entertainment (gaming, cinema), and user-generated content (UGC)/passthrough. 3 representative HDR videos were selected for each category, each of which was manually mastered using Nuke⁶ on our haploscope to span the dynamic range of our reference display (1,000 nits, 1M:1 contrast).

Naïve sampling of videos, e.g. if overrepresented by those with high average luminance, could skew user preferences. As such, we attempted to sample videos which span a wide distribution of luminances, as shown in Figure 5, with some bright videos (e.g. Porsche, Werewolf) and others with very high contrast (e.g. Showgirl, Smith). UGC/Passthrough videos were from the SJTU HDR video sequence dataset [Song et al. 2016] and the Smith, Showgirl scenes were collected from the HdM-HDR-2014 sequences [Froehlich et al. 2014]. The rest of our content is original – Face videos were captured using a RED Komodo digital camera⁷, Productivity content created in Unity, and the Werewolf scene modeled in Blender. All videos were encoded with HDR10 metadata (4K, 60fps, 10-bit, BT. 2100 primaries, PQ EOTF). Additional details are described in Supplement E.

The 12 scenes are tone-mapped to 5 different peak luminance values and 5 different contrast ratios using the two TMOs described in Section 3.2. In total, this amounts to $12 \text{ scenes} \times (5 \text{ peak luminances} \times 5 \text{ contrasts} \times 2 \text{ TMOs} + 1 \text{ reference}) = 612 \text{ videos}$. The contrast and luminance parameters are spaced logarithmically due to the nonlinear perception of light by the human visual system:

- Peak luminance [nits]: 63, 125, 250, 500, 1,000
- Contrast: 64:1, 320:1, 1,600:1, 8,000:1, 40,000:1.

⁶Nuke software product site: [foundry.com/products/nuke-family/nuke](https://www.foundry.com/products/nuke-family/nuke)

⁷RED Komodo product site: red.com/komodo

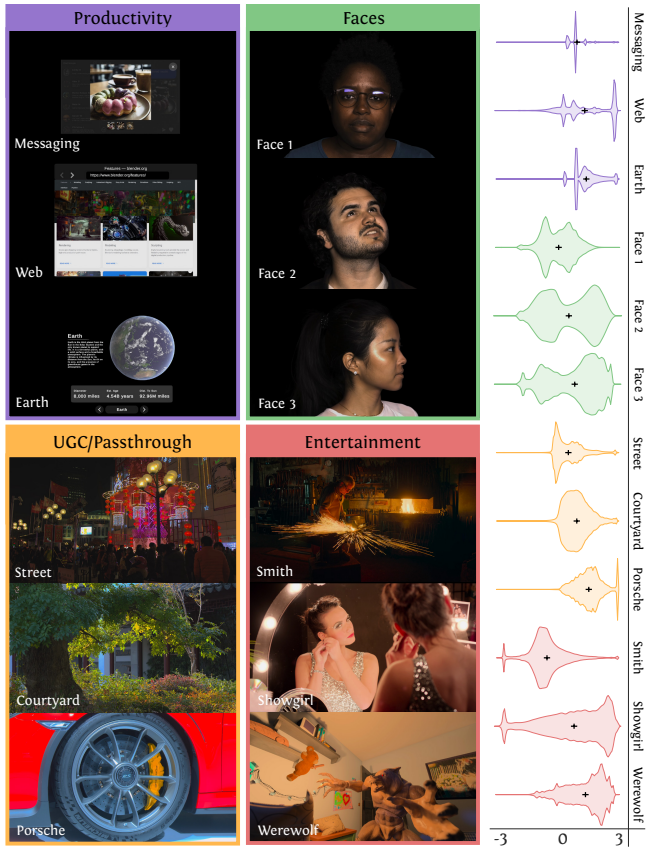


Figure 5: HDR video stimuli. We presented users 12 HDR videos in total, grouped into 4 content types. Representative frames are displayed. Luminance distributions (x -axis in log nits) aggregated over all frames are visualized as violin plots, grouped by category. Note that in the Productivity and Faces scenes, the black background is discounted in the luminance plots. Image credits HdM-Stuttgart, SJTU, Blender.

The reference is pegged at 1,000,000:1 contrast and 1,000 nits peak luminance (our haploscope’s limit, and the original master of the content). Example stimuli are displayed in Supplement Section A.3.

3.4 User Study

Finally, our large-scale user study was conducted using tone-mapped (Section 3.2) HDR video stimuli (Section 3.3) displayed on our haploscope testbed (Section 3.1).

Participants. We recruited 41 paid participants (ages 24–61), all of which had normal or corrected-to-normal vision. Color deficiency was assessed using the Ishihara test, but users who failed parts of the test (3 users in total) were not excluded as their data was not significantly different from the other participants (see Section 4). An Institutional Review Board (IRB) approved the study, and all participants signed consent forms before beginning the experiment.

Experimental Procedure. Our experimental design consisted of a two-interval forced choice (2IFC) task using the method of paired

comparisons, as forced-choice protocols were found to lead to less noisy data compared to rating-based studies (e.g. Likert scale) [Mantiuk et al. 2012] by presenting a simpler task to users.

Each trial in our experiment began by showing the user the reference condition. Participants used a three-key keyboard to switch between this and two tone-mapped test videos, and were not able to proceed to the next trial until all three videos were viewed at least once. A selection was made by pressing on a foot pedal. A 500ms gray screen at the mean luminance of the incoming stimulus was included when switching to prevent direct comparisons between conditions. This also helped ensure appropriate luminance adaptation for each incoming stimulus, as it is longer than the required bright-to-bright saturation time [Hayhoe et al. 1987].

Participants were seated for the duration of the study, and perceived stimuli through our haploscope testbed. The lights in the room were turned off for the duration of the study to mitigate glare, and to simulate an environment representative of enclosed VR HMDs. A chinrest was used to stabilize users’ heads and align their eyes with the viewing mirrors. Participants were instructed to select the video which is closer to the reference, in terms of both contrast and brightness. A 15-second timer was included, but time constraints were not enforced. Before the start of each study, a 4-trial training session is conducted to familiarize users with the study setup and stimuli. Each scene used in the study session was shown to users during the training.

Stimuli Sampling. In total, our study consists of 612 unique stimuli (see Section 3.3 for the calculation). We allowed comparisons between all parameters except across scenes. A naïve full study design would amount to $\binom{612}{2} = 186,966$ pairwise comparisons, which is prohibitively large. Instead, we used the active sampling ASAP framework [Mikhailiuk et al. 2021] to determine the optimal conditions to probe in each trial. Given all previous responses, ASAP determines comparisons providing the maximum expected information gain. To further reduce participant workload, we split the study into 4 sessions, with each user rating 3 out of 12 scenes, resulting in $612/4 = 153$ trials (one for each condition). On average, participants spent 30.8 minutes to complete the active portion of the study. The experiment logic and HDR video presentation were implemented using PsychToolbox 3 [Kleiner et al. 2007].

4 Results

The data from our psychophysical study was converted to a unified perceptual Just-Objectionable-Difference (JOD) scale using Bayesian maximum likelihood estimation assuming observers behave according to Thurstone’s Case V model [Thurstone 2017]. We used the *pwcmp*⁸ algorithm [Perez-Ortiz and Mantiuk 2017] to perform this statistical scaling procedure, and to filter outlier observers with an inter-quartile-normalised score above 1.5 (2 were removed). We point readers to the work of Perez-Ortiz and Mantiuk [2017] for an in-depth definition of the JOD unit. JODs can also be converted to percentage preference (see Supplementary Figure 14). If display A has a score 1 JOD greater than B, this means display A would be selected 75% of the time over display B; if A has score 2 JODs greater than B, it would be selected 91% of the time and so on.

⁸*pwcmp* library: github.com/mantiuk/pwcmp

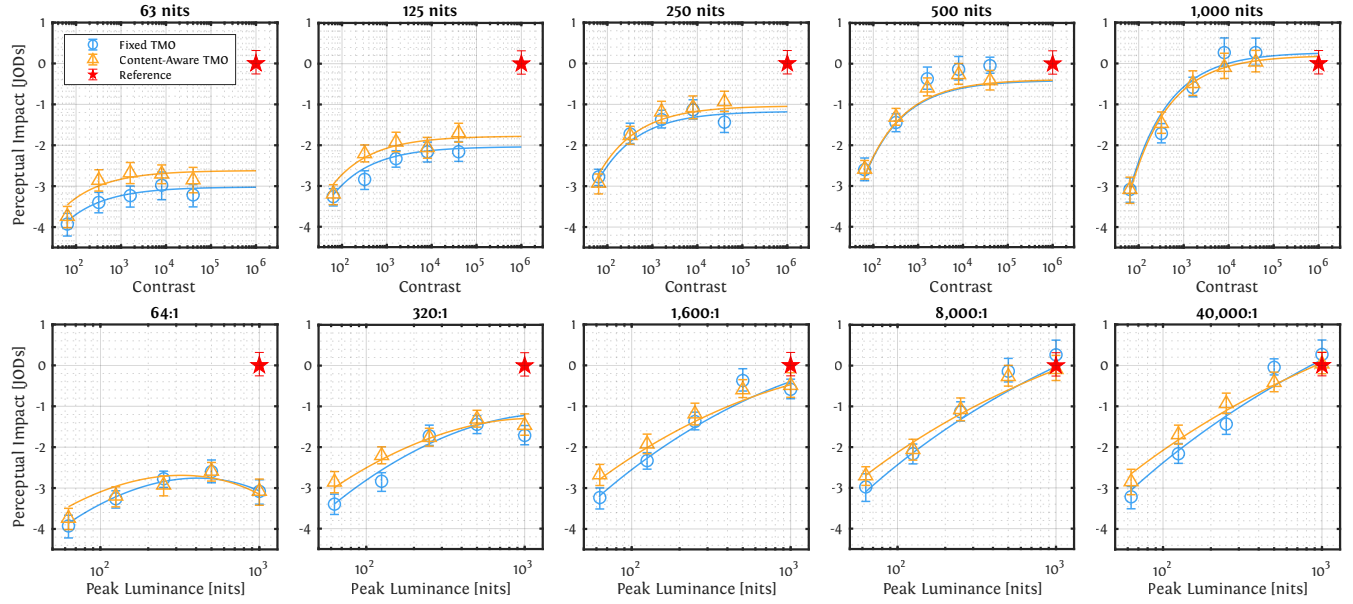
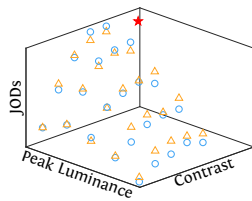


Figure 6: User study results. Our data contains 3 axes – contrast, peak luminance (nits), and perceptual impact (JODs). We display these results as a projection onto the contrast (first row) and peak luminance (second row) axes. Each individual plot here represents iso-contrast/peak luminance data. For example, in the top left figure, the x -axis is contrast and the y -axis is perceptual impact for constant 63 nit peak luminance. Error bars represent 95% confidence intervals. The red star is the reference condition, which itself has an error bar because it was a condition in the user study. Orange triangles are the results for the CONTENT-AWARE TMO, and blue circles represent the FIXED TMO. Each plot's x -axis is on a log scale. Solid lines are model evaluations for each TMO.

A preview of the study results (aggregated across scenes), parameterized by contrast, peak luminance (nits), and perceptual impact (JODs) for the two tone mappers we studied (FIXED TMO: \circ , CONTENT-AWARE TMO: \triangle), is shown in the inset. A detailed projection of the 3D data along the two studied axes is shown in Figure 6. Error bars represent the range of scaled JOD scores which lie within a 95% confidence interval, computed by simulating 1,000 bootstrap samples using *pwcmp*. The reference (red star, 1,000 nits, 1M:1 contrast) is pegged to 0 JODs; note that the JOD scale is relative, and score differences represent the perceived distance between two conditions. Tabulated JOD values are shown in Supplement B.

Qualitatively, we note that for increases in both contrast and peak luminance, JOD scores increase but seem to plateau for high values ($>1,000:1$ contrast and 500 nit peak luminance). However, for high peak luminances and very low contrast, scores decrease; this is likely because of the very high black level (>15 nits for a 1,000 nit, 64:1 contrast display) in these conditions. The same trend was observed in earlier work by Seetzen et al. [2006]. An N-way analysis of variance (ANOVA) was conducted on the aggregate results to determine the main effects of all study variables on JOD scores. The analysis found significant main effects on JOD scores for contrast ($p \ll 0.01$), peak luminance ($p \ll 0.01$), and tone mapping ($p = 0.0046$). Additionally, a significant interaction effect was observed between peak luminance and tone mapping ($p = 0.0034$), but not



between contrast and tone mapping ($p = 0.1372$). This is likely explained by the fact that our TMO compresses the highlight only, so differences in tone mapping technique are more apparent for displays with lower peak luminance, while black level is treated the same for both methods. A per-video analysis found the main effect of video category was not significant ($p = 0.99$), but significant interaction effects between video category and contrast ($p \ll 0.01$), peak luminance ($p \ll 0.01$), and TMO ($p = 0.0039$) were found.

5 Model

We fit an analytical model to the data collected from our perceptual study to predict JOD scores given black level and peak luminance. Black level is modeled after findings that sensitivity follows the square root of luminance at low light levels [de Vries 1943; Rose 1948] while peak luminance is modeled as a logarithmic function following Weber's law,

$$f(L_{\min}) = k_1 - k_2 \sqrt{L_{\min}} \quad (4)$$

$$g(L_{\max}) = \log_{10}(L_{\max})^{k_3} \quad (5)$$

$$\mathcal{M}(L_{\min}, L_{\max}) = f(L_{\min}) \cdot g(L_{\max}) - k_4, \quad (6)$$

where $\mathcal{M} : \mathbb{R}^2 \rightarrow \mathbb{R}$, L_{\min} is black level, and L_{\max} is peak luminance of the display. The fitted parameters of our model $k_{1,\dots,4}$ are displayed in Supplement C. Note that both Equation (4) and Equation (5) behave monotonically with respect to decreases in L_{\min} and increased L_{\max} , but the multiplication of the two in Equation (6) can result in lower JOD scores for a combination of high L_{\min} and

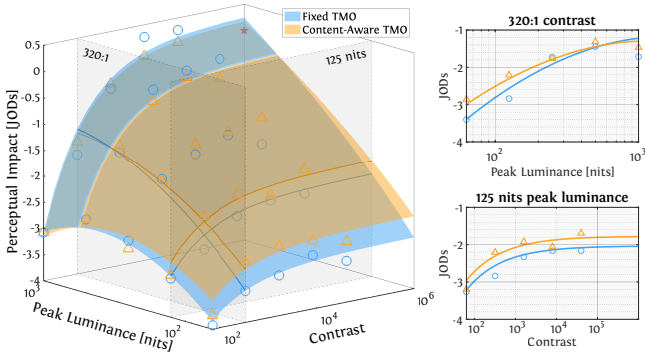


Figure 7: Computational model. An analytical model is fit to our user study data (FIXED TMO: \circ , CONTENT-AWARE TMO: \triangle), and rendered as a 3D surface for both TMOs we studied. Slices of the surface, one at constant 320:1 contrast and the other at 125 nits, are plotted at the intersection of grey planes and shown to right. Scatter points are scaled user study data.

high L_{\max} (low contrast, high peak luminance), which is a trend we hoped to capture given the same observation in our study data.

Our model fit has a root mean square error (RMSE) of 0.23 and 0.16 (measured vs. predicted JOD scores) for the FIXED TMO and CONTENT-AWARE TMO, respectively. A render of the 3D surface fit is shown in Figure 7, and slices along each axis are to the right. In Fig. 6 and Supplement Section C.1, we plot slices for all conditions.

5.1 Subjective Model Evaluation

A study with 12 additional participants (ages 22–45, 7 male) was conducted to validate that our model generalizes to a headmounted VR scenario. This study employed different scenes, tested different display parameters, and followed a new experiment protocol from the main study to ensure thorough validation of the model.

As commercially available VR headsets have significant limitations in terms of contrast and peak luminance, we opted to use a custom HDR VR HMD prototype. Our headset is similar to the one described by Matsuda et al. [2022b]. An achromatic doublet is placed in the viewing path, so the dynamic range of the content is distorted based on its characteristics. Because no standard protocol exists for VR metrology that would accurately capture this effect, we employed a custom process. Simultaneous contrast is found by measuring the luminance of a checkerboard test pattern with varying spatial frequencies, using a CS-2000 spectroradiometer. Contrast was defined by the luminance measurement of a white divided by a black checker, and found to be between 45:1 and 340,000:1 depending on spatial frequency of the measured pattern. The peak luminance of the display was 1,000 nits for all measurements.

To get a representative value of simultaneous contrast for stimuli used in our study, we performed a through-the-lens measurement of the luminance of 3° white and black square patches placed in a bright region of each scene (see Figure 8, right). Contrast measurements were made for scenes tone-mapped to 60, 250, and 750 nits peak luminance using the FIXED TMO. Exact measurement data are displayed in Section G.3. The contrast variable plugged into our

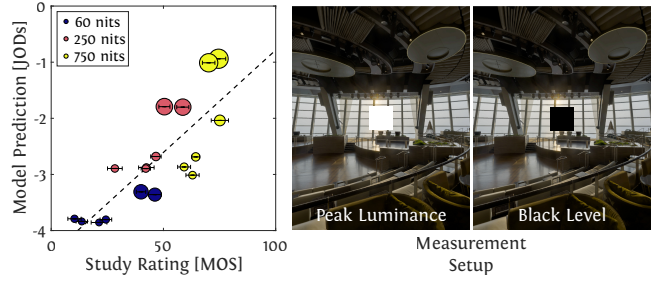


Figure 8: Validation study results and measurement. User study results (left) are displayed, with study rating (MOS) on the x -axis, and model predictions (JOD) on the y -axis. Scatter colors represent peak luminance, and larger markers correspond to higher scene contrast. Horizontal error bars represent standard deviation of scores (SOS). The contrast of each scene displayed in HDR VR was found by measuring the luminance of a 3° square (right). Image credit Greg Zaal.

model for this validation correspond to these ground-truth measurements for the 3 peak luminances, rather than via simulation of black level as done in the main study.

Six 360° HDRI probes (Supplement Section G.2) were used in our study. In total, we have $(6 \text{ scenes}) \times (3 \text{ peak luminances}) = 18$ conditions. We conducted 4 repeats for each trial, following the recommendations of Perez-Ortiz and Mantiuk [2017], for a total of 72 trials per user. To make tone-mapped stimuli viewable in real-time with head tracking, we stored the FIXED TMO as a lookup table implemented as a Unity shader (see Supplement Section G.4).

We followed the ITU P.910 standard for rating-based studies [Installations and Line 1999]. A user is first presented with the reference HDRI (1,000 nits peak luminance), and is able to switch between it and a tone-mapped scene. Participants were allowed to view scenes as they wish, with natural head movements. After viewing both images, the user is then asked to rate the test image with respect to the reference on a five-point scale.

Ratings averaged across repeats were converted to mean opinion scores (MOS) using the Netflix Sureal library [Li and Bampis 2017; Li et al. 2020]. Figure 8 shows the resulting MOS scores plotted against the JOD scores predicted by our model. Linear (Pearson $r = 0.813, p \ll .01$) and rank-order (Spearman $\rho = 0.820, p \ll .01$) correlations between study ratings and model predictions are strong [Moore and Kirkland 2007], indicating that our model can predict the results of the headmounted VR setting validation study well. Further discussion can be found in Supplement G.

6 Applications

In this section, we describe some practical applications of our model.

6.1 Predicting Display Quality

Given a display’s peak luminance and contrast, our model can predict its subjective quality score (in JOD units). This is demonstrated in Figure 9, where a JOD score is predicted for all parameter combinations. Iso-JOD contours are plotted at 0.5 JOD steps, or around a

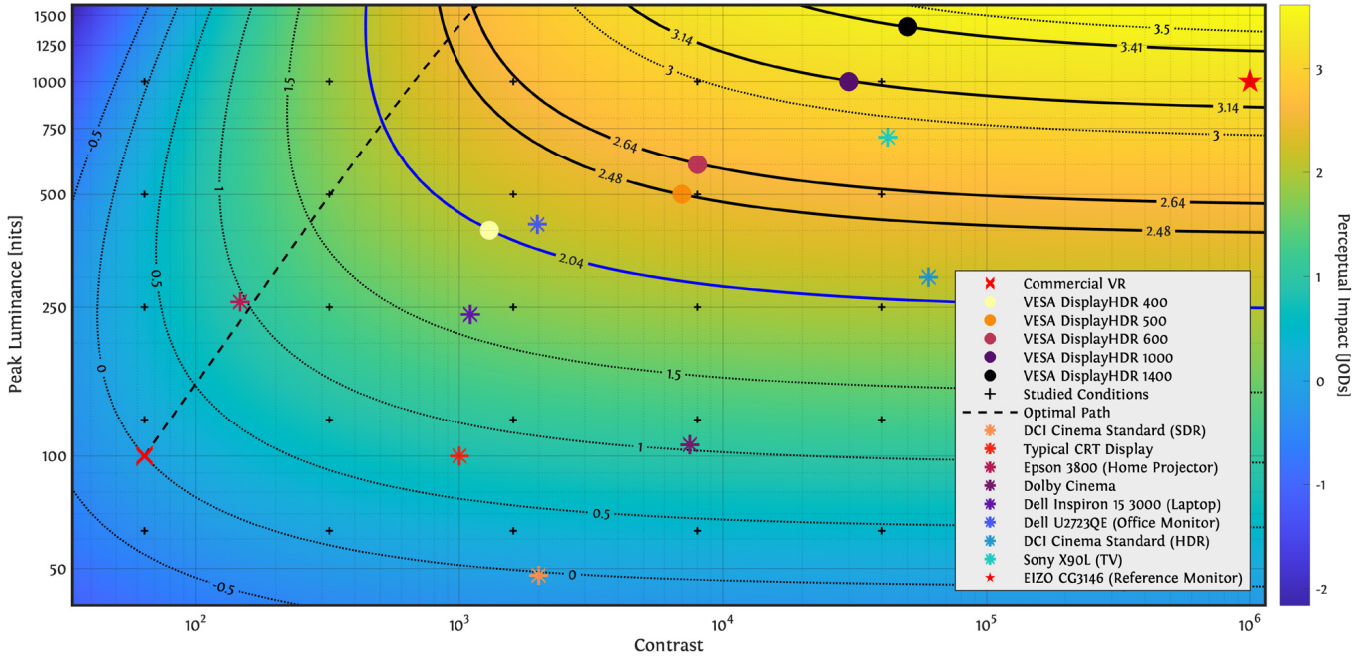


Figure 9: Display quality predicted by our model. Our computational model (fit to the CONTENT-AWARE TMO data) is evaluated for all combinations of peak luminance and contrast to create a plot of iso-JOD contours. The conditions sampled in our user study are plotted as black crosses. Here, the baseline (0 JODs, red X) is set to parameters plausible for commercial VR display (100 nits, 64:1 contrast). Iso-JOD contours are plotted at 0.5 JOD steps, and for 5 tiers in the VESA DisplayHDR standard (circle points). An optimal path (dashed line) along the model’s gradient is plotted, starting from the baseline. Several additional display technologies are plotted as asterisks, and the reference monitor used in our study as a red star.

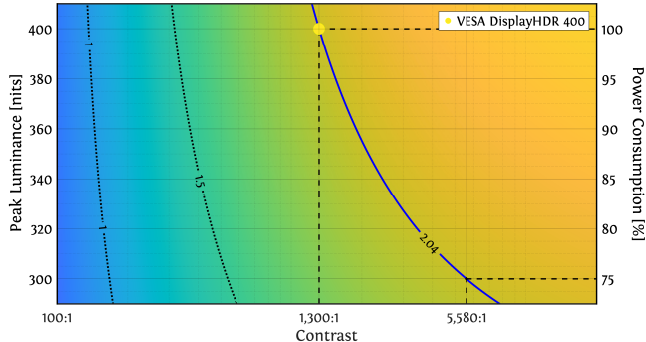


Figure 10: Iso-JOD contours. A curve evaluated at constant JOD value (here 2.04 JODs) is plotted as a blue line. The intersections of this contour line at 100% and 75% power consumption, assuming a reference display with VESA DisplayHDR 400 parameters (400 nits, 1,300:1), are plotted as dashed lines.

63.2% preference. Note that the baseline is set to plausible parameters for a commercial VR display (100 nits, 64:1) [Mehrfard et al. 2019]. Similarly, we can predict the expected perceptual quality of each tier in the VESA DisplayHDR standard. A set of commercially available non-VR displays are plotted for reference (asterisks), including theater projectors, TVs, laptops displays, and monitors,

enabling perceptual comparisons between different display technologies and standards (see Supplement H for details).

6.2 Design Tradeoffs

Commercial display design involves evaluating tradeoffs in performance, production cost, power consumption, etc. For example, if designing a VR headset with the goal of improving the commercial VR baseline in our plot by 2 JOD units (approx. VESA DisplayHDR 400); combinations of contrast and peak luminance which satisfy this improvement are plotted as a blue curve in Figure 9, with a zoom-in plotted in Figure 10. As an example, a display with 400 nits peak and 1,300:1 contrast would provide this improvement, but so would one with 300 nits peak and 5,580:1 contrast. If prioritizing battery life, the option with lower peak luminance may be preferable. However, the latter choice may be more appealing if optical elements that allow for high contrast are expensive to manufacture.

For standalone VR headsets, power consumption is especially important: up to 40% of an XR device’s power is consumed by the display component [Anand et al. 2011]. We paired our display quality model with the LCD display power usage prediction defined by Chen et al. [2024]. In Figure 10, we show that reducing the peak luminance of a reference display (yellow marker) will consume proportionately less power, but to compensate for the loss of visual quality and maintain a constant JOD score, contrast must be increased, with black level reduced from 0.3 nits to 0.05 nits.

7 Limitations & Future Work

ISO-JOD curves for traditional displays were evaluated using our model, given contrast and luminance. In addition, while our study simulated VR with HDR monitors in a haploscope setting, the effect of viewing conditions, optics, etc. would have to be assessed. This work could serve as a framework for future study targeting traditional displays, which could confirm our model's generalizability.

Our display simulation uniform black level increase which is realistic for LCD displays, but only approximates the effects of VR optics on the content. In our validation study, we showed our model works for VR HDR with optics, but contrast had to be measured per scene, which is impractical for large-scale application. Future improvements to VR metrology and optical modeling would allow our model to be applied to arbitrary VR optics scenarios. In addition, exploring the perceptual trade-offs of different backlight or optical architectures would be an interesting follow-up to this work.

Our study employed a practical tone mapping pipeline, following modern recommendations. A very different TMO may lead to altered results, in which case it may be useful to repeat this study.

8 Conclusion

We conducted a large-scale psychophysical study on subjective preferences in VR, measuring the impact of peak luminance and contrast, the two main variables defining HDR display. Our study quantified the preference for higher peak luminance and contrast, and suggested that preference saturates at high values. These results were captured via a computational model, which was validated with a second subjective study. Finally, we discussed how this model can be used to evaluate display standards, guide display design, and quantify trade-offs between quality and display power.

Acknowledgments

We thank Ken Koh for creating HDR productivity content and Maurizio Nitti for rendering and designing HDR teddy bear scenes. Thanks to Dennis Pak for designing/constructing the haploscope and the mirror setup. Calibration of the EIZO display could not have been accomplished without the support of Yuta Asano. Thank you to Ben Mills for building the enclosure of our haploscope, for calibration of displays, as well as binocular calibration and alignment of mirrors. Thanks go to Will McCann and Xin Li, who supported the construction of the hardware and mirror fabrication. This project would not have been successful without the support of Fartun Sheygo and Alex Gherman, who conducted the main study, Nour Shoora who organized it, the user study participants for their time, and John Hill and Romain Bachy for help with logistics. Thanks go to Henry Milani for providing a PR-745 for validation of our displays, and Reza Saeedpour for support with using the device. Thank you to Dounia Hammou for providing pointers to HDR video datasets, Professor Rafał Mantiuk for the many discussions related to tone mapping and more, and Daryn Blanc-Goldhammer for comments on our work. We are grateful to Alexis Terterov for conducting the validation study, and EIZO support team for help debugging HDR displays. Thanks to Doug Lanman for discussions. Finally, thank you to Jenna Kang, Niall Williams, and Colin Groth for help with figure style. This work is partially supported by National Science Foundation grant #2225861, and a DARPA ICS program.

References

- Ahmet Oundefineduz Akyüz, Roland Fleming, Bernhard E. Riecke, Erik Reinhard, and Heinrich H. Büthoff. 2007. Do HDR displays support LDR content? a psychophysical evaluation. *ACM Trans. Graph.* 26, 3 (July 2007), 38–es. <https://doi.org/10.1145/1276377.1276425>
- Bhajan Anand, Karthik Thirugnanam, Jeena Sebastian, Pravein G. Kannan, Akhilhebal L. Ananda, Mun Choon Chan, and Rajesh Krishna Balan. 2011. Adaptive display power management for mobile games. In *Proceedings of the 9th International Conference on Mobile Systems, Applications, and Services* (Bethesda, Maryland, USA) (*MobiSys '11*). Association for Computing Machinery, New York, NY, USA, 57–70. <https://doi.org/10.1145/1999995.2000002>
- Malika Ashraf, Rafal Mantiuk, Jasna Martinovic, and Sophie Wuergler. 2022. Suprathreshold Contrast Matching between Different Luminance Levels. *Color and Imaging Conference* 30, 1 (2022), 219–219. <https://doi.org/10.2352/CIC.2022.30.1.38>
- Alexandre Chapiro, Dongyeon Kim, Yuta Asano, and Rafal K. Mantiuk. 2024. ARDAVID: Augmented Reality Display Artifact Video Dataset. *ACM Trans. Graph.* 43, 6, Article 186 (Nov. 2024), 11 pages. <https://doi.org/10.1145/3687969>
- Alexandre Chapiro, Timo Kunkel, Robin Atkins, and Scott Daly. 2018. Influence of Screen Size and Field of View on Perceived Brightness. *ACM Trans. Appl. Percept.* 15, 3, Article 18 (July 2018), 13 pages. <https://doi.org/10.1145/3190346>
- Alexandre Chapiro, Nathan Matsuda, Malika Ashraf, and Rafal Mantiuk. 2023. Critical flicker frequency (CFF) at high luminance levels. *Electronic Imaging* 35 (2023), 1–5.
- Bin Chen, Akshay Jindal, Michal Piováří, Chao Wang, Hans-Peter Seidel, Piotr Didyk, Karol Myszkowski, Ana Serrano, and Rafal K. Mantiuk. 2023. The effect of display capabilities on the gloss consistency between real and virtual objects. In *SIGGRAPH Asia 2023 Conference Papers* (Sydney, NSW, Australia) (*SA '23*). Association for Computing Machinery, New York, NY, USA, Article 90, 11 pages. <https://doi.org/10.1145/3610548.3618226>
- Kenneth Chen, Thomas Wan, Nathan Matsuda, Ajit Ninan, Alexandre Chapiro, and Qi Sun. 2024. PEA-PODs: Perceptual Evaluation of Algorithms for Power Optimization in XR Displays. *ACM Trans. Graph.* 43, 4, Article 67 (jul 2024), 17 pages. <https://doi.org/10.1145/3658126>
- Scott Daly, Timo Kunkel, Xing Sun, Suzanne Farrell, and Poppy Crum. 2013. Preference limits of the visual dynamic range for ultra high quality and aesthetic conveyance. In *Human Vision and Electronic Imaging XVIII*, Bernice E. Rogowitz, Thrasyvoulos N. Pappas, and Huub de Ridder (Eds.), Vol. 8651. International Society for Optics and Photonics, SPIE, 86510J. <https://doi.org/10.1117/12.2013161>
- H.L. de Vries. 1943. The quantum character of light and its bearing upon threshold of vision, the differential sensitivity and visual acuity of the eye. *Physica* 10, 7 (1943), 553–564. [https://doi.org/10.1016/S0031-8914\(43\)90575-0](https://doi.org/10.1016/S0031-8914(43)90575-0)
- G. Eilertsen, R. K. Mantiuk, and J. Unger. 2017. A comparative review of tone-mapping algorithms for high dynamic range video. *Comput. Graph. Forum* 36, 2 (May 2017), 565–592. <https://doi.org/10.1111/cgf.13148>
- E. S. Ferry. 1892. Persistence of vision. *American Journal of Science* s3-44, 261 (sep 1 1892), 192–207. <https://doi.org/10.2475/ajs.s3-44.261.192>
- James Ferwerda. 2001. Elements of early vision for computer graphics. *IEEE computer graphics and applications* 21, 5 (2001), 22–33.
- Jan Froehlich, Stefan Grandinetti, Bernd Eberhardt, Simon Walter, Andreas Schilling, and Harald Brendel. 2014. Creating cinematic wide gamut HDR-video for the evaluation of tone mapping operators and HDR-displays. In *Digital Photography X*, Nitin Sampat, Radka Tezaur, Sebastiano Battiatto, and Boyd A. Fowler (Eds.), Vol. 9023. International Society for Optics and Photonics, SPIE, 90230X. <https://doi.org/10.1117/12.2040003>
- Dounia Hammou, Lukáš Krasula, Christos G. Bampis, Zhi Li, and Rafał K. Mantiuk. 2024. The effect of viewing distance and display peak luminance — HDR AV1 video streaming quality dataset. In *2024 16th International Conference on Quality of Multimedia Experience (QoMEX)*. 193–199. <https://doi.org/10.1109/QoMEX61742.2024.10598289>
- M.M. Hayhoe, N.I. Benimoff, and D.C. Hood. 1987. The time-course of multiplicative and subtractive adaptation process. *Vision Research* 27, 11 (1987), 1981–1996. [https://doi.org/10.1016/0042-6989\(87\)90062-9](https://doi.org/10.1016/0042-6989(87)90062-9)
- Telephone Installations and Local Line. 1999. Subjective video quality assessment methods for multimedia applications. *Networks* 910, 37 (1999), 5.
- M Kleiner, D Brainard, Denis Pelli, A Ingling, R Murray, and C Broussard. 2007. What's new in psychtoolbox-3. *Perception* 36, 14 (2007), 1–16.
- J.J. Kulikowski. 1976. Effective contrast constancy and linearity of contrast sensation. *Vision Research* 16, 12 (1976), 1419–1431. [https://doi.org/10.1016/0042-6989\(76\)90161-9](https://doi.org/10.1016/0042-6989(76)90161-9)
- Timo Kunkel and Erik Reinhard. 2010. A reassessment of the simultaneous dynamic range of the human visual system. In *Proceedings of the 7th Symposium on Applied Perception in Graphics and Visualization* (Los Angeles, California) (*APGV '10*). Association for Computing Machinery, New York, NY, USA, 17–24. <https://doi.org/10.1145/1836248.1836251>
- Zhi Li and Christos G. Bampis. 2017. Recover Subjective Quality Scores from Noisy Measurements. In *2017 Data Compression Conference (DCC)*. 52–61. <https://doi.org/10.1109/DCC.2017.26>

- Zhi Li, Christos G. Bampis, Lucjan Janowski, and Ioannis Katsavounidis. 2020. A Simple Model for Subject Behavior in Subjective Experiments. *Electronic Imaging* 32, 11 (2020), 131–1–131–1. <https://doi.org/10.2352/ISSN.2470-1173.2020.11.HVEI-131>
- Rafal Mantiuk, Scott Daly, and Louis Kerofsky. 2010. The luminance of pure black: exploring the effect of surround in the context of electronic displays. In *Human Vision and Electronic Imaging XV*, Bernice E. Rogowitz and Thrasyvoulos N. Pappas (Eds.), Vol. 7527. International Society for Optics and Photonics, SPIE, 75270W. <https://doi.org/10.1117/12.840549>
- Rafal K. Mantiuk, Param Hanji, Malika Ashraf, Yuta Asano, and Alexandre Chapiro. 2024. ColorVideoVDP: A visual difference predictor for image, video and display distortions. *ACM Trans. Graph.* 43, 4, Article 129 (July 2024), 20 pages. <https://doi.org/10.1145/3658144>
- Rafal K. Mantiuk, Anna Tomaszewska, and Radoslaw Mantiuk. 2012. Comparison of Four Subjective Methods for Image Quality Assessment. *Comput. Graph. Forum* 31, 8 (Dec. 2012), 2478–2491. <https://doi.org/10.1111/1467-8659.2012.03188.x>
- Nathan Matsuda, Alex Chapiro, Yang Zhao, Clinton Smith, Romain Bachy, and Douglas Lanman. 2022a. Realistic Luminance in VR. In *SIGGRAPH Asia 2022 Conference Papers* (Daegu, Republic of Korea) (SA '22). Association for Computing Machinery, New York, NY, USA, Article 21, 8 pages. <https://doi.org/10.1145/3550469.3555427>
- Nathan Matsuda, Yang Zhao, Alex Chapiro, Clinton Smith, and Douglas Lanman. 2022b. HDR VR. In *ACM SIGGRAPH 2022 Emerging Technologies* (Vancouver, BC, Canada) (SIGGRAPH '22). Association for Computing Machinery, New York, NY, USA, Article 4, 2 pages. <https://doi.org/10.1145/3532721.3535566>
- Arian Mehrfard, Javad Fotouhi, Giacomo Taylor, Tess Forster, Nassir Navab, and Bernhard Fuerst. 2019. A comparative analysis of virtual reality head-mounted display systems. *arXiv preprint arXiv:1912.02913* (2019).
- Aliaksei Mikhailiuk, Clifford Wilmot, Maria Perez-Ortiz, Dingcheng Yue, and Rafal K. Mantiuk. 2021. Active Sampling for Pairwise Comparisons via Approximate Message Passing and Information Gain Maximization. In *2020 25th International Conference on Pattern Recognition (ICPR)*. 2559–2566. <https://doi.org/10.1109/ICPR48806.2021.9412676>
- Scott Miller, Mahdi Nezamabadi, and Scott Daly. 2013. Perceptual Signal Coding for More Efficient Usage of Bit Codes. *SMPTE Motion Imaging Journal* 122 (05 2013), 52–59. <https://doi.org/10.5594/j18290>
- David S Moore and Stephane Kirkland. 2007. *The basic practice of statistics*. Vol. 2. WH Freeman New York.
- Yongmin Park and Michael J. Murdoch. 2020. Image quality equivalence between peak luminance and chromaticity gamut. *Journal of the Society for Information Display* 28, 11 (2020), 854–871. <https://doi.org/10.1002/jsid.906>
- Maria Perez-Ortiz and Rafal K Mantiuk. 2017. A practical guide and software for analysing pairwise comparison experiments. *arXiv preprint arXiv:1712.03686* (2017).
- Thomas Conrad Porter. 1902. Contributions to the study of flicker. Paper II. *Proceedings of the Royal Society of London* 70, 459-466 (1902), 313–329.
- Ana Radonjić, Sarah R. Allred, Alan L. Gilchrist, and David H. Brainard. 2011. The Dynamic Range of Human Lightness Perception. *Current Biology* 21, 22 (2011), 1931–1936. <https://doi.org/10.1016/j.cub.2011.10.013>
- Erik Reinhard, Michael Stark, Peter Shirley, and James Ferwerda. 2002. Photographic tone reproduction for digital images. *ACM Trans. Graph.* 21, 3 (July 2002), 267–276. <https://doi.org/10.1145/566654.566575>
- Allan G. Rempel, Wolfgang Heidrich, Hiroe Li, and Rafal Mantiuk. 2009. Video viewing preferences for HDR displays under varying ambient illumination. In *Proceedings of the 6th Symposium on Applied Perception in Graphics and Visualization* (Chania, Crete, Greece) (APGV '09). Association for Computing Machinery, New York, NY, USA, 45–52. <https://doi.org/10.1145/1620993.1621004>
- Albert Rose. 1948. The Sensitivity Performance of the Human Eye on an Absolute Scale*. *J. Opt. Soc. Am.* 38, 2 (Feb 1948), 196–208. <https://doi.org/10.1364/JOSA.38.000196>
- Christophe Schlick. 1995. Quantization Techniques for Visualization of High Dynamic Range Pictures. In *Photorealistic Rendering Techniques*, Georgios Sakas, Stefan Müller, and Peter Shirley (Eds.). Springer Berlin Heidelberg, Berlin, Heidelberg, 7–20.
- Helge Seetzen, Wolfgang Heidrich, Wolfgang Stuerzlinger, Greg Ward, Lorne Whitehead, Matthew Trentacoste, Abhijeet Ghosh, and Andrejs Vorozcovs. 2004. High dynamic range display systems. *ACM Trans. Graph.* 23, 3 (Aug. 2004), 760–768. <https://doi.org/10.1145/1015706.1015797>
- Helge Seetzen, Hiroe Li, Linton Ye, Wolfgang Heidrich, Lorne Whitehead, and Greg Ward. 2006. 25.3: Observations of luminance, contrast and amplitude resolution of displays. In *SID Symposium Digest of Technical Papers*, Vol. 37. Wiley Online Library, 1229–1233.
- BT Series. 2019. Methods for conversion of high dynamic range content to standard dynamic range content and vice-versa. (2019).
- Li Song, Yankai Liu, Xiaokang Yang, Guangtao Zhai, Rong Xie, and Wenjun Zhang. 2016. The SJTU HDR Video Sequence Dataset. In *Proceedings of International Conference on Quality of Multimedia Experience (QoMEX 2016)*. Lisbon, Portugal, 2. tex.ids=Song.2016.SHv
- Lothar Spillmann and John S Werner. 2012. *Visual perception: the neurophysiological foundations*. Elsevier.
- SMPTE Standard. 2014. High dynamic range electro-optical transfer function of mastering reference displays. *SMPTE ST 2084*, 2014 (2014), 11.
- Taimoor Tariq, Nathan Matsuda, Eric Penner, Jerry Jia, Douglas Lanman, Ajit Ninan, and Alexandre Chapiro. 2023. Perceptually Adaptive Real-Time Tone Mapping. In *SIGGRAPH Asia 2023 Conference Papers* (Sydney, NSW, Australia) (SA '23). Association for Computing Machinery, New York, NY, USA, Article 36, 10 pages. <https://doi.org/10.1145/3610548.3618222>
- Louis L Thurstone. 2017. A law of comparative judgment. In *Scaling*. Routledge, 81–92.
- Jack Tumblin and Holly Rushmeier. 1993. Tone Reproduction for Realistic Images. *IEEE Comput. Graph. Appl.* 13, 6 (Nov. 1993), 42–48. <https://doi.org/10.1109/38.252554>
- Peter Vangorp, Karol Myszkowski, Erich W. Graf, and Rafal K. Mantiuk. 2015. A model of local adaptation. *ACM Trans. Graph.* 34, 6, Article 166 (nov 2015), 13 pages. <https://doi.org/10.1145/2816795.2818086>
- Robert Wanat, Josselin Petit, and Rafal Mantiuk. 2012. Physical and Perceptual Limitations of a Projector-based High Dynamic Range Display. In *Theory and Practice of Computer Graphics*, Hamish Carr and Silvester Czanner (Eds.). The Eurographics Association. <https://doi.org/10.2312/LocalChapterEvents/TPCG/TPCG12/009-016>
- Greg Ward. 2008. Defining dynamic range. In *ACM SIGGRAPH 2008 Classes* (Los Angeles, California) (SIGGRAPH '08). Association for Computing Machinery, New York, NY, USA, Article 30, 3 pages. <https://doi.org/10.1145/1401132.1401173>
- Krzysztof Wolski, Fangcheng Zhong, Karol Myszkowski, and Rafal K. Mantiuk. 2022. Dark stereo: improving depth perception under low luminance. *ACM Trans. Graph.* 41, 4, Article 146 (July 2022), 12 pages. <https://doi.org/10.1145/3528223.3530136>